

Supporting Information for:

Raman Fingerprints of Amyloid Structures

*Jessica D. Flynn and Jennifer C. Lee**

Laboratory of Protein Conformation and Dynamics, Biochemistry and Biophysics Center,
National Heart, Lung, and Blood Institute, National Institutes of Health
Bethesda, MD 20892 United States

*Email: leej4@mail.nih.gov, Phone: (301) 827-0723

Contents:

- Experimental Methods
- Figure S1: Comparison of soluble and aggregated forms of N-acetyl α -syn, ApoCIII, and RPT₃₁₅₋₄₄₄.
- Figure S2: Expanded view of amide-I band for fibrillar RPT₃₁₅₋₄₄₄ showing peak at 1733 cm^{-1} indicative of protonated glutamic acid.
- Figure S3: Raman mapping of Het-S₂₁₈₋₂₈₉ showing original Raman spectra for three spatial location indicated in map.

Experimental Methods

Chemicals— Sodium chloride ($\geq 99.5\%$), sodium acetate trihydrate ($\geq 99.5\%$), sodium phosphate monobasic ($\geq 99.0\%$), sodium phosphate dibasic ($\geq 99.0\%$), ethylenediaminetetraacetic acid (EDTA) ($\geq 99\%$), hydrochloric acid (36.5%–38%), cyclohexane (anhydrous, 99.8%), phenylmethanesulfonyl fluoride (PMSF) ($\geq 98.5\%$), and thioflavin-T (ThT) were purchased from Sigma-Aldrich and used as received. Ultra pure tris(hydroxymethyl)aminomethane (Tris) and guanidine hydrochloride (GuHCl) were purchased from MP Biomedicals.

Recombinant Protein Expression, Purification, and Preparation— N-acetyl α -syn, RPT₃₁₅₋₄₄₄, and ApoCIII were expressed and purified as previously described.¹ Het-S₂₁₈₋₂₈₉ plasmid² was a generous gift from Reed Wickner (NIDDK, NIH) and expressed in BL21(DE3) pLysS cells (Invitrogen). Het-S₂₁₈₋₂₈₉ cell pellet from a 2-L culture was resuspended into 30 mL 6 M GuHCl, 100 mM Na₂HPO₄, 100 mM NaCl, 10 mM imidazole, pH 8.2, and gently agitated at 4 °C overnight. Soluble lysate was separated by centrifugation (30 min, Sorvall, SS-34 rotor, 18,000 rpm, 4 °C) and incubated with 5 mL of equilibrated Ni-NTA agarose resin (Qiagen) for 1 hr at 4 °C with gentle agitation. Unbound protein was washed from the column using 4×10 mL aliquots of pH 7 buffer (10 mM NaPi, 4 M urea, 100 mM NaCl, 20 mM imidazole), followed by elution of bound protein using 7×1.5 mL aliquots of pH 7 buffer (10 mM NaPi, 4 M urea, 100 mM NaCl, 200 mM imidazole). Fractions were analyzed by SDS-PAGE and visualized by Coomassie blue staining. Het-S₂₁₈₋₂₈₉ containing fractions were pooled and further purified by cationic exchange chromatography using a Mono-S 10/100 column (GE Healthcare).

A β _{M1-40} was expressed in BL21(DE3) pLysS cells (Invitrogen) and purified using a modified procedure from previously reported protocols.⁴ Cell pellet from a 2-L culture was resuspended in 50 mL of lysis buffer (10 mM Tris, 1 mM EDTA, 8 M urea, pH 8) and then subjected to three freeze/thaw cycles, followed by probe-tip sonication on ice (2 min cycles until lysate was optically clear). The soluble fraction was separated from cell debris by centrifugation (30 min, Beckman Coulter, 45Ti rotor, 30,000 rpm, 4 °C), added to 50 mL of DEAE-resin (GE Healthcare, DEAE Sepharose, Fast Flow) equilibrated in buffer A (10 mM Tris, 1 mM EDTA, pH 8), and gently agitated overnight at 4 °C. The slurry was added to a 60-mL fritted glass funnel (coarse) and the resin was washed with 50 mL buffer A, followed by stepwise elution using 50 mL aliquots of buffer A with 25 mM NaCl ($\times 2$), 125 mM NaCl ($\times 5$), and 250 mM NaCl ($\times 2$), using gentle vacuum for collection of fractions. Fractions were analyzed by SDS-PAGE and visualized by Coomassie blue staining. Fractions containing highest amounts of A β _{M1-40} were further purified by gel filtration chromatography on a HiLoad 16/60 Superdex 75 (GE Healthcare) equilibrated with pH 7.4 buffer (10 mM sodium phosphate). All samples were evaluated by SDS-PAGE/silver-staining methods and mass spectrometry (NHLBI Biochemistry Core Facility).

To form fibrils, protein solutions were exchanged into either pH 5 buffer (10 mM sodium acetate (NaOAc) and 100 mM NaCl) or pH 7.4 buffer (10 mM sodium phosphate (NaPi) and 100 mM NaCl) using a PD-10 column (GE Healthcare) immediately prior to aggregation. Protein concentration was determined by UV-visible spectroscopy (ϵ_{280} (N-acetyl α -syn) = 5120 M⁻¹ cm⁻¹; ϵ_{280} (RPT₃₁₅₋₄₄₄) = 5500 M⁻¹ cm⁻¹; ϵ_{280} (ApoCIII) = 19,480 M⁻¹ cm⁻¹; ϵ_{280} (Het-S) = 6990 M⁻¹ cm⁻¹; ϵ_{275} (A β _{M1-40}) = 1400 M⁻¹ cm⁻¹) using a CARY Bio300 prior to aggregation. Protein samples were incubated ([N-acetyl α -syn] = 30 μ M and [RPT₃₁₅₋₄₄₄] = 30 μ M at pH 5; [ApoCIII] = 10 μ M, [A β _{M1-40}] = 18 μ M, and [Het-S₂₁₈₋₂₈₉] = 40 μ M at pH 7.4) in 1.5 mL Eppendorf tubes at 37 °C and shaken at 600 rpm (Mini-Micro 980140 shaker, VWR) for 3–10 days.

ThT Emission Assay— Small aliquots of aggregated proteins were taken from Eppendorf tubes and diluted to final concentration of 5 μ M protein, then incubated with 10 μ M ThT for 30 min at RT. ThT

fluorescence was measured in a micro-quartz cuvette (Starna) at 25 °C using a Horiba Fluorolog-3 spectrofluorimeter ($\lambda_{\text{ex}} = 410$ nm, $\lambda_{\text{obs}} = 450\text{--}600$ nm, 0.25 s integration time, 1 and 2 nm excitation and emission slit widths, respectively). ThT intensity for each protein was then integrated from 450 nm to 550 nm and plotted for comparison.

TEM— Aggregated protein samples (10 μL) were incubated on TEM grids (400-mesh Formvar carbon coated copper, Electron Microscopy Sciences) for 1–2 minute. Sample solution was wicked with filter paper and grid was quickly washed with water (10 μL) to remove any excess material and improve background contrast (except RPT₃₁₅₋₄₄₄ samples). Grids were then incubated with 1% (w/v) aqueous uranyl acetate (UA) solution (10 μL) for 30–60 s. Excess UA was wicked away with filter paper and grids were air dried. TEM images were collected using a JOEL JEM 1200EX TEM (accelerating voltage 80 keV) equipped with an AMT XR-60 digital camera (NHLBI EM Core Facility).

Raman Spectroscopy— All data were collected at RT in an 8-well #1 coverglass LabTek chamber (a 10–20 μL droplet) using the 514-nm line of an Ar-ion laser (CVI Melles Griot, ~ 65 mW at the sample) coupled to an inverted microscope (Olympus IX71) as previously described⁵ with the following modifications. A 400- μm pinhole (Thorlabs) has been added at the imaging plane before the spectrometer (Horiba Scientific, iHR 320) and a Märzhäuser Wetzler motorized XYZ-stage (SCAN IM 120 \times 80, Tango controller) was used. Data were collected using a 1200 gr/mm grating and a liquid-N₂ cooled back illuminated deep-depletion CCD array (Horiba Scientific, Symphony II, 1 MHz repetition rate with high gain enabled, no data binning). Typically, 25 spectra from 500–3700 cm^{-1} of 3–5 s acquisition time were taken for each sample. For mapping, 2.5–3 μm step sizes were taken. The bright field image was collected using a USB 2.0 camera (iDS, UI-1220-C). Neat cyclohexane (20 μL in a sealed capillary tube) was used for calibration each day. Bandpass and accuracy were found to be <12 cm^{-1} and ± 1 cm^{-1} , respectively. Raman spectra were corrected by subtracting buffer backgrounds and applying a baseline polynomial fit (Lab Spec 6 software). Second derivative analysis was performed using the *differentiate operation* IGOR Pro 7 (Wavemetrics), which calculates the 1D numerical derivative of a wave (our Raman spectrum). By executing this operation twice, we calculate the second derivative of each spectrum and objectively identify changes from positive to negative slope, enabling characteristic spectral component differences in the vibrational bands to be precisely located. From this analysis, the negative maximum of the second derivative identifies the maximum intensity frequency for a spectral region. We chose second derivative analysis over other methods of spectral deconvolution because it offers an unbiased analysis, with no assumptions made on the number of components present in each spectrum. For more information on this approach, we encourage the reader to refer to the following literature examples: C. Balestrieri, G. Colonna, A. Giovane, G. Irace and L. Servillo, *Eur. J. Biochem.*, **1978**, *90*, 433-440; S. Heino and D. M. Byler, *Biochem. Biophys. Res. Commun.*, **1983**, *115*, 391 - 397.

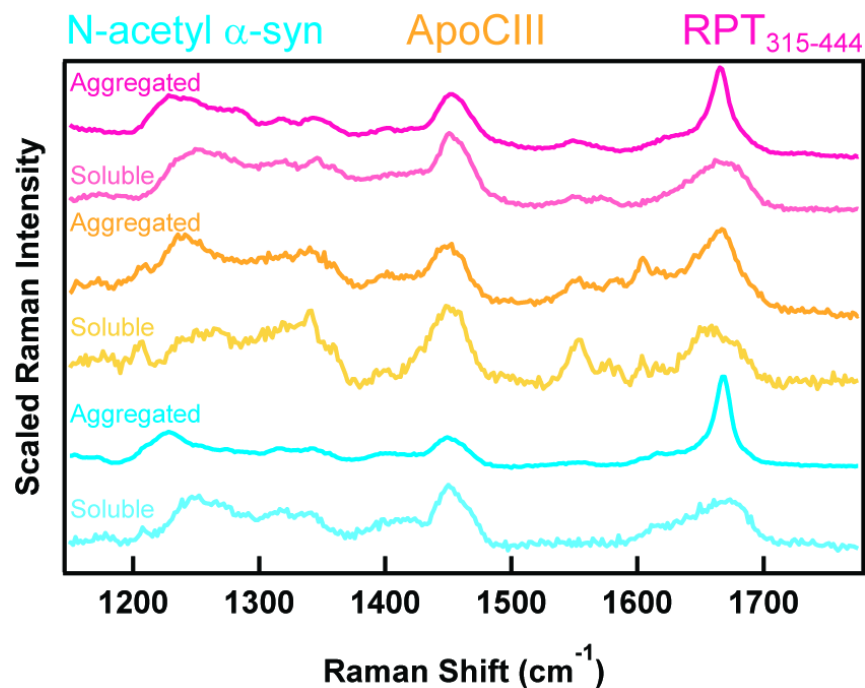


Figure S1. Comparison of soluble and aggregated forms of N-acetyl α -syn, ApoCIII, and RPT₃₁₅₋₄₄₄. The sharpening of the amide-I band between 1650–1700 cm⁻¹ is a clear indication of β -sheet structure and the formation of amyloid structure. Additionally, shifts of the amide-III band between 1200–1300 cm⁻¹ to lower energies is an indication of β -sheet structure and the formation of amyloid structure. We did not measure the soluble forms of A β _{M1-40} and Het-s₂₁₈₋₂₈₉ due to their extremely rapid aggregation.

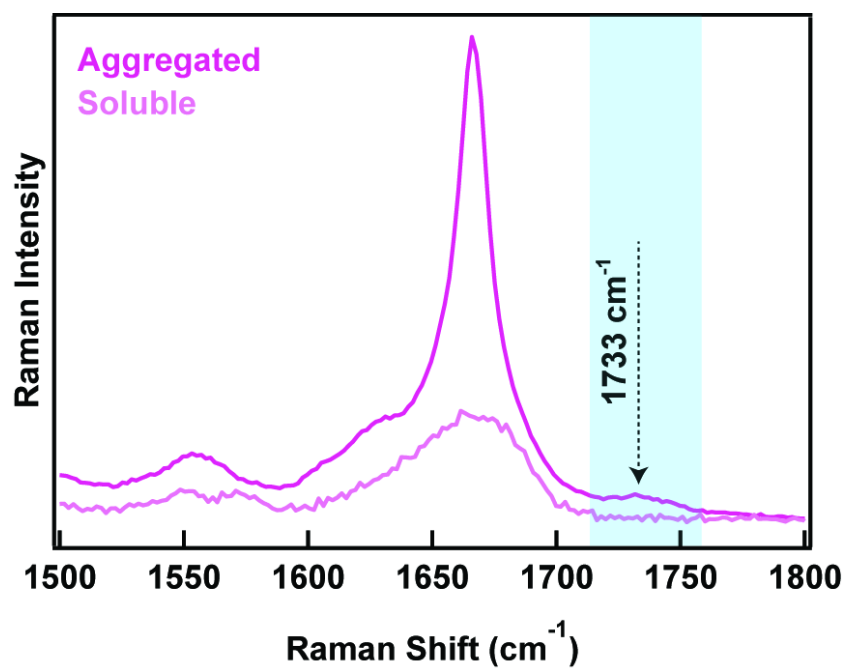


Figure S2. Expanded view of soluble and aggregated RPT₃₁₅₋₄₄₄. A broad peak centered at 1733 cm⁻¹, indicative of protonated glutamic acid, is observed in the aggregated form, but absent in the soluble form. Protonation of glutamic acid is a known requirement for RPT₃₁₅₋₄₄₄ fibril formation.³

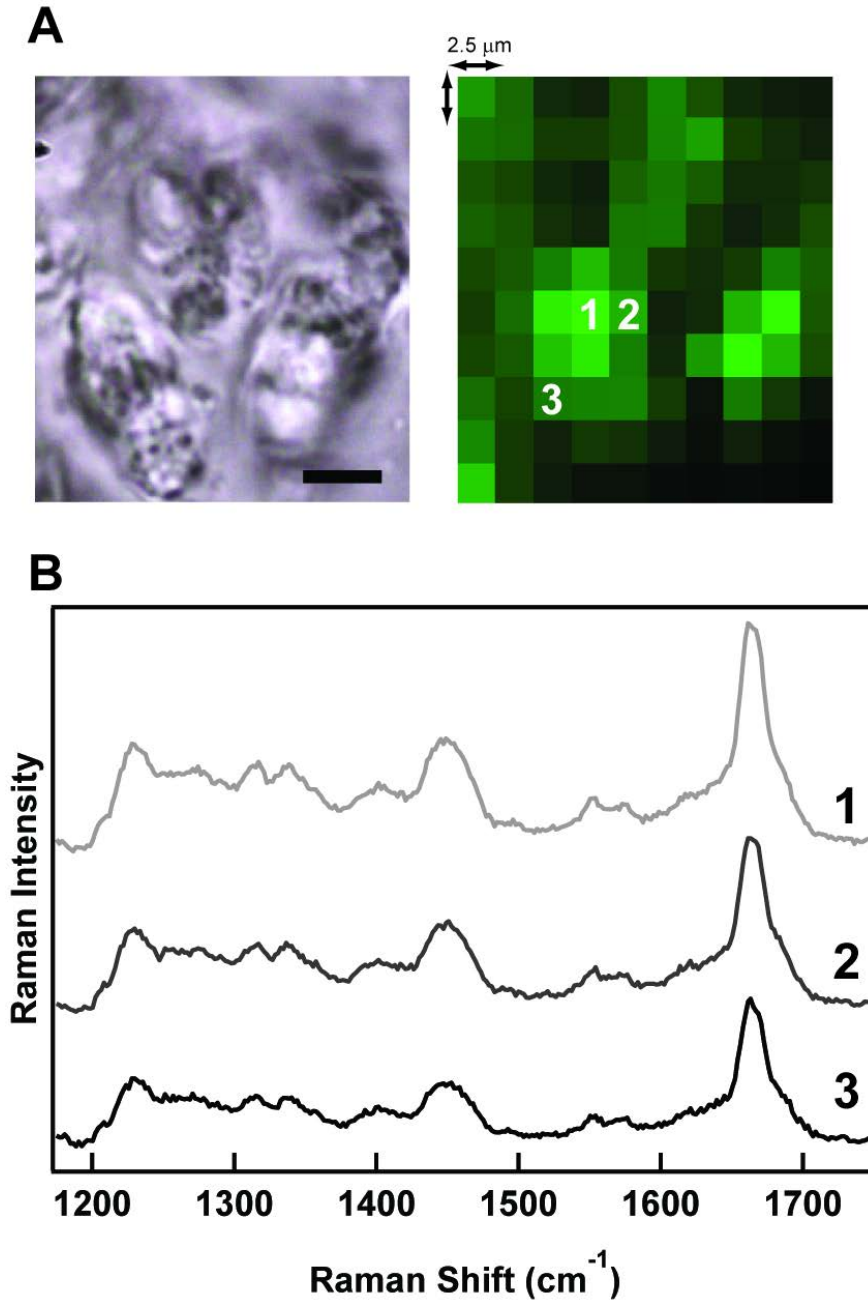


Figure S3. Raman mapping of Het-s₂₁₈₋₂₈₉ showing original Raman spectra for three spatial location indicated in map.

References

1. (a) R. P. McGlinchey, G. A. Dominah and J. C. Lee, *Biochemistry*, 2017, **56**, 3881-3884; (b) Z. Jiang and J. C. Lee, *J Mol Biol*, 2014, **426**, 4074-4086; (c) C. A. Brisbois and J. C. Lee, *Biochemistry*, 2016, **55**, 4939-4948.
2. B. Chen, K. R. Thurber, F. Shewmaker, R. B. Wickner and R. Tycko, *Proc Natl Acad Sci U S A*, 2009, **106**, 14339-14344.
3. R. P. McGlinchey, Z. Jiang and J. C. Lee, *Chembiochem*, 2014, **15**, 1569-1572.
4. D. M. Walsh, E. Thulin, A. M. Minogue, N. Gustavsson, E. Pang, D. B. Teplow and S. Linse, *FEBS J*, 2009, **276**, 1266-1281.
5. J. D. Flynn, R. P. McGlinchey, R. L. Walker, 3rd and J. C. Lee, *J Biol Chem*, 2018, **293**, 767-776.